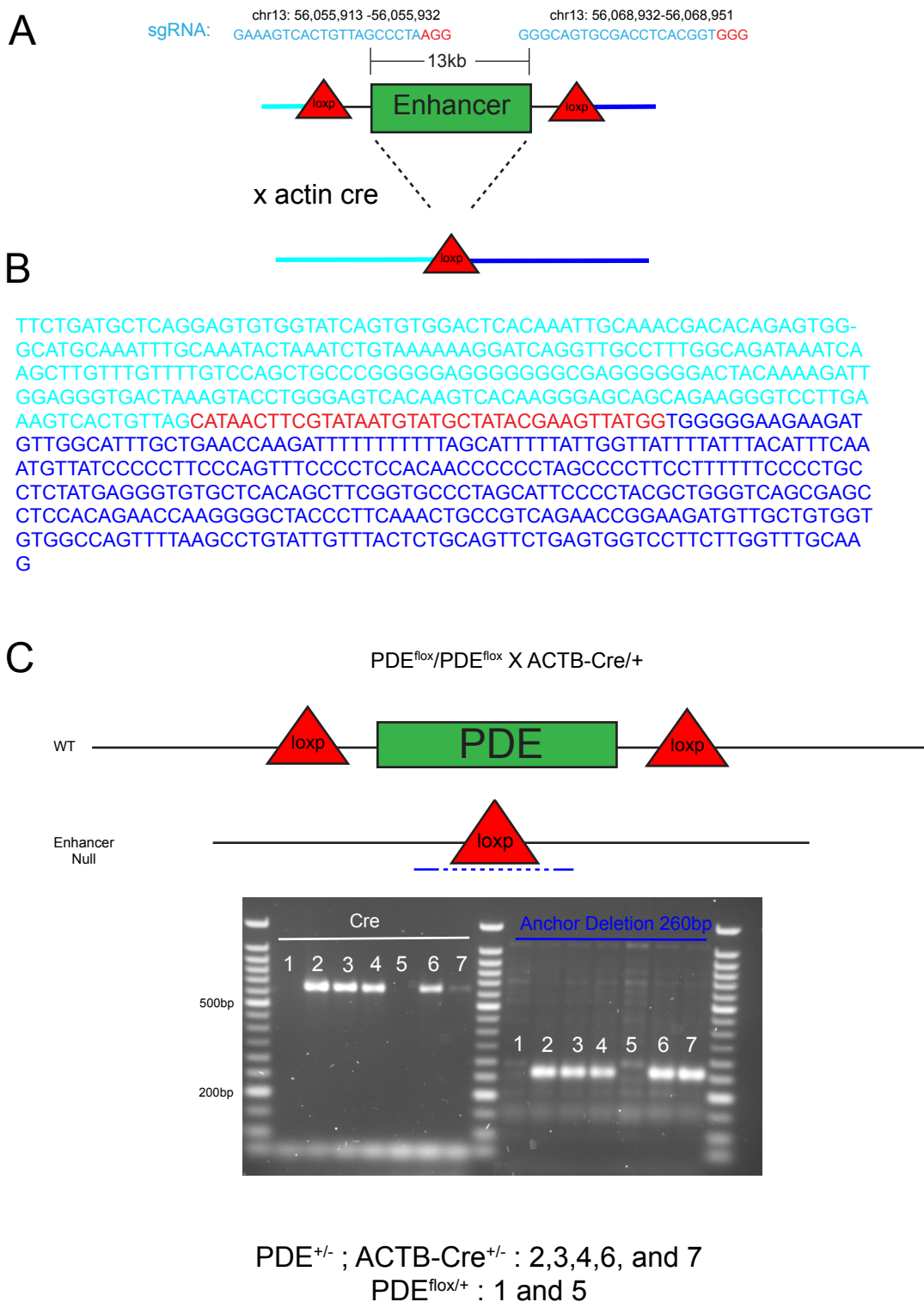


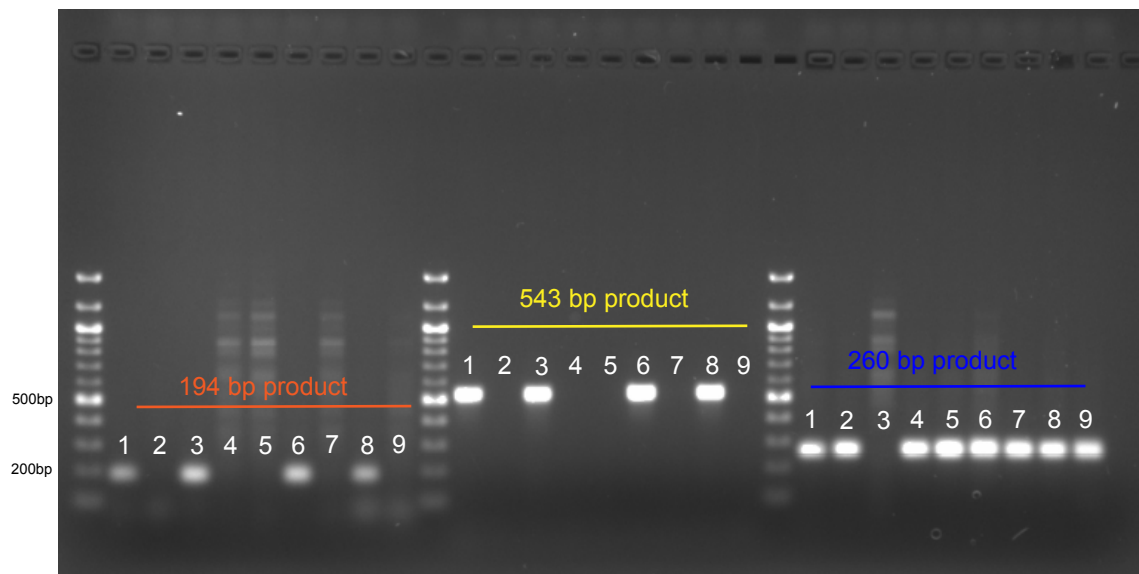
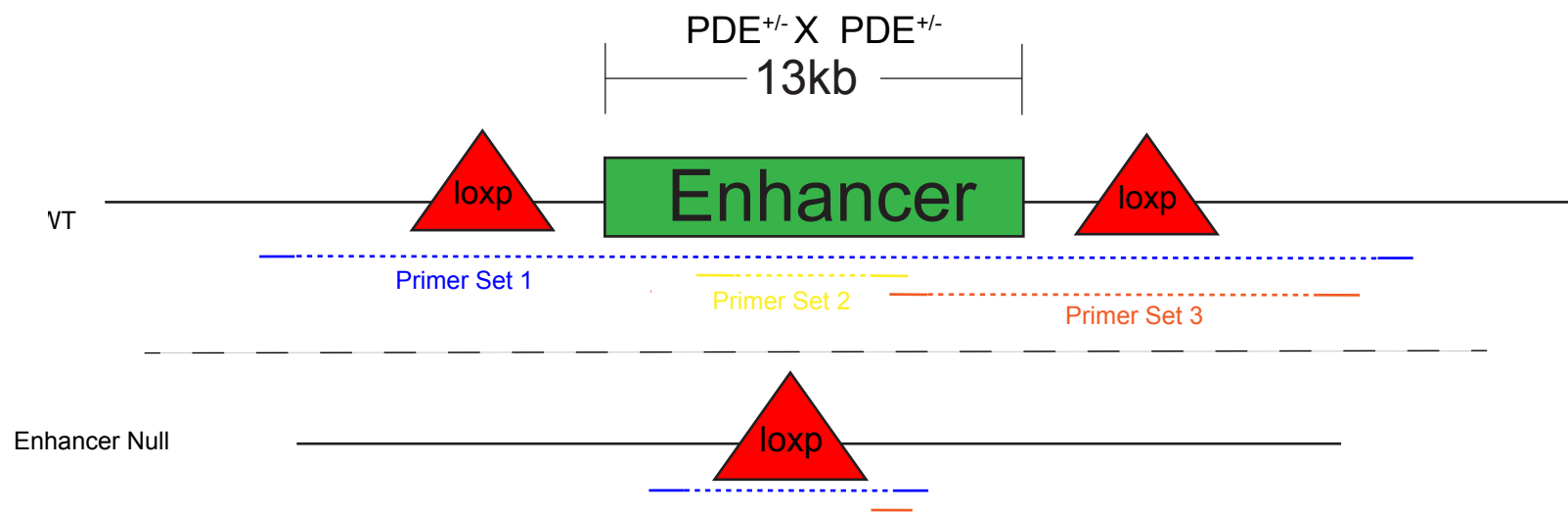
Figure S1.



**Figure S1. Generation and validation of the PDE deletion allele.**

A. *Top*. Schematic illustrating the location of the PDE (green) and flanking loxP sites (red). The sgRNA sequences used for genome editing are shown at the top of the figure with the PAM sites highlighted in red (chr13: 56,055,913 -56,055,932 ; chr13: 56,068,932-56,068,951; mm9). *Bottom*. Mice with a floxed PDE allele were crossed with Actin-Cre mice to generate the constitutive PDE knockout line (also see panel C). B. Validation of the PDE deletion allele using Sanger sequencing. After Cre recombination, a single loxP sequence (in red) remains. Genomic sequence immediately 5' of the PDE is shown in light blue (chr13: 56,055,668-56,055,927), and sequence immediately 3' of the PDE is shown in dark blue (chr13: 56,068,951-56,069,282). C. PCR genotyping to identify PDE<sup>+/-</sup> offspring resulting from the PDE<sup>flx</sup>/flx x ACTb-cre<sup>+/+</sup> cross used to generate the PDE constitutive knockout line. A 260 bp PCR amplicon (in blue) spanning the remaining loxP site was used to detect PDE deletion alleles. A 680 bp PCR amplicon was used to detect the presence of the ACTb-cre allele. PDE deletion alleles were only detected in mice carrying ACTb-cre (lanes 2, 3, 4, 6 and 7).

**Figure S2.**

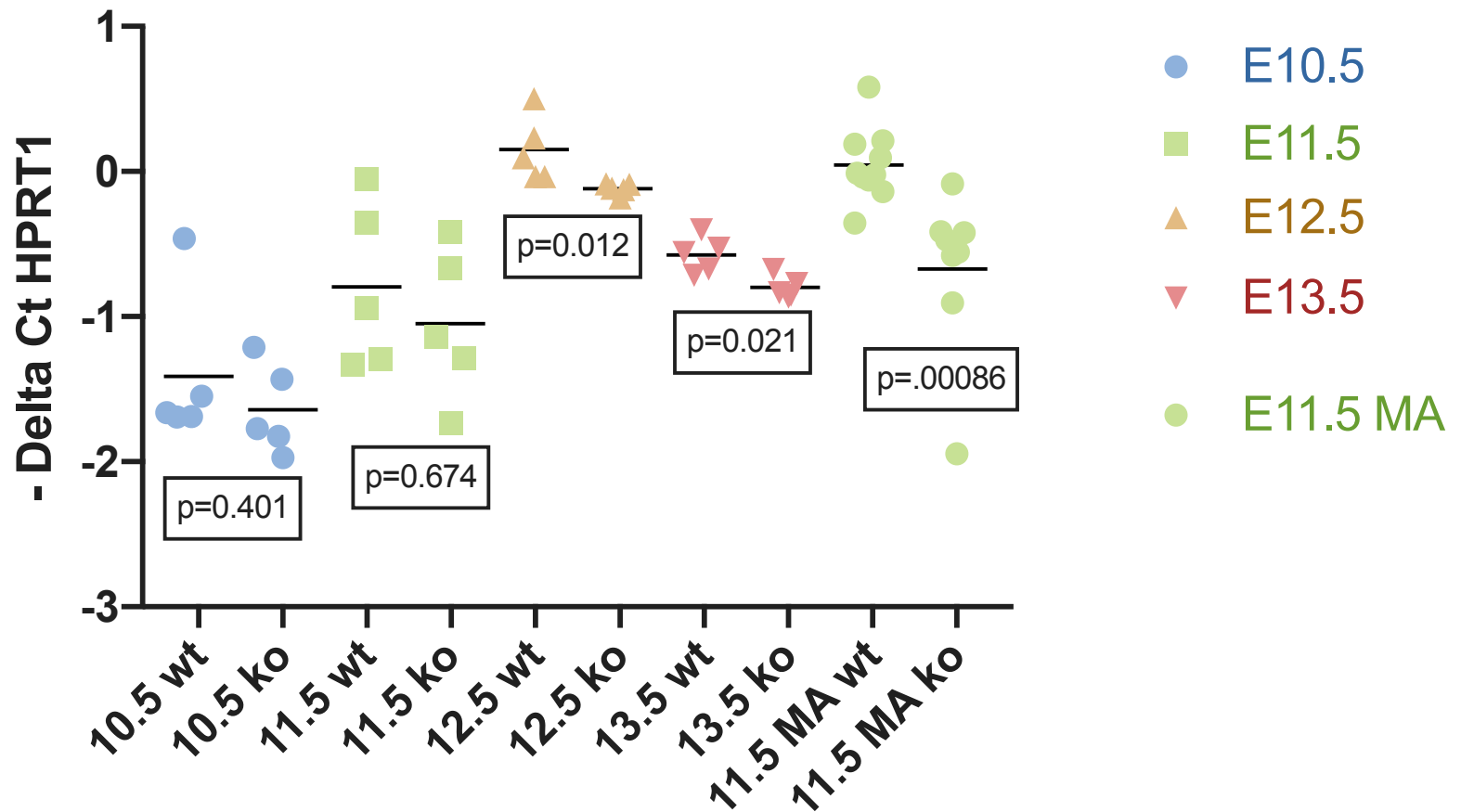


PDE<sup>+/+</sup> Mice: 3  
PDE<sup>+/-</sup> Mice: 1, 6, AND 8  
PDE<sup>-/-</sup> Mice: 2, 4, 5, 7, and 9

**Figure S2. Genotyping strategy.**

A. Schematic representation of the three PCR primer sets used to distinguish wild type, heterozygous, and homozygous PDE deletion mice. Primer set 1 (blue) spans the 13 kb PDE and produces a 260 bp product in PDE<sup>+/-</sup> and PDE<sup>-/-</sup> mice, but not wild type mice. Primer set 2 (yellow) is located within the PDE and produces a 543 bp product in wild type and PDE<sup>+/-</sup> mice, but not PDE<sup>-/-</sup> mice. Primer set 3 (orange) spans the junction between the PDE and flanking genomic sequence and produces a 194 bp product in wild type and PDE<sup>+/-</sup> mice, but not PDE<sup>-/-</sup> mice. B. Representative genotyping assay; lanes corresponding to mice of each genotype are indicated below the gel image.

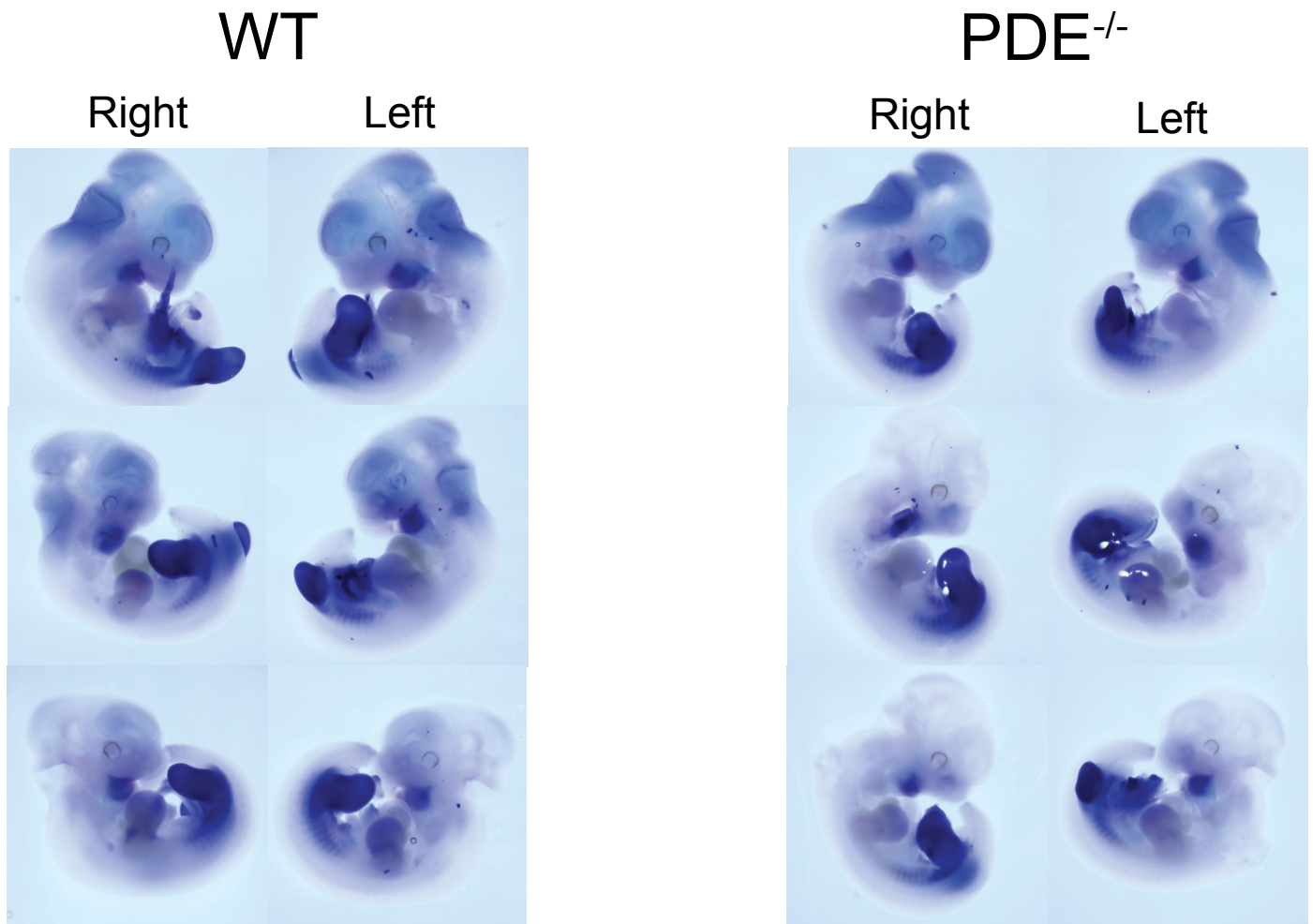
Figure S3.



**Figure S3. Comparing *Pitx1* expression in hindlimb and mandibular arch in litter-matched wild type and PDE<sup>-/-</sup> mice.**

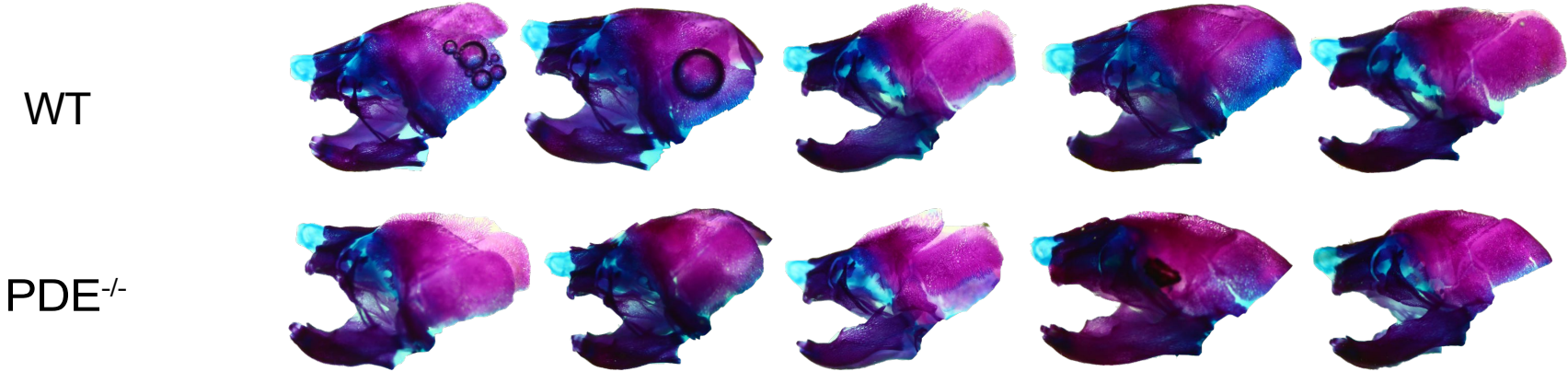
*Pitx1* expression was compared across samples using *Hprt1* expression as an internal reference. The vertical axis shows  $-(Ct)$  values, calculated as  $-(Ct_{Pitx1} - Ct_{HPRT1})$ . Ct values were converted to  $-(Ct)$  values for purposes of illustration, but were not used for statistical testing. Each data point at each developmental stage represents a litter-matched, one-to-one measure of *Pitx1* expression in wild type ('wt') or PDE<sup>-/-</sup> ('ko') mouse. These measurements were used to generate the summary data shown in Figure 2. Differential expression P values were calculated for each tissue and timepoint using a Mann-Whitney U test.

Figure S4.



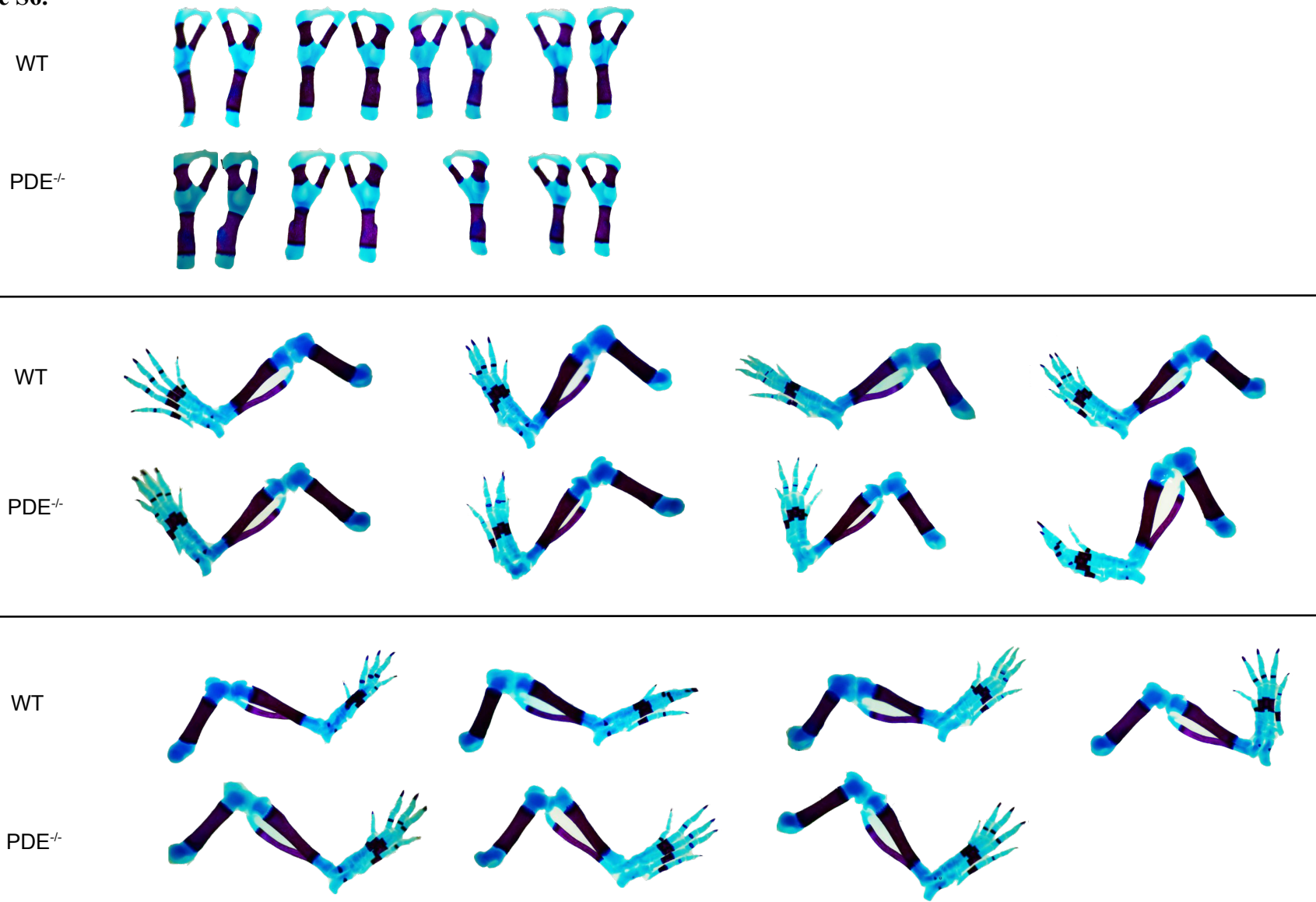
**Figure S4. Comparison of *Pitx1* expression in wild type and PDE<sup>-/-</sup> E11.5 embryos using whole mount *in situ* hybridization.** Additional examples presented in support of results shown in Figure 3.

Figure S5.



**Figure S5. Comparison of E18.5 skull morphology in wild type and PDE<sup>-/-</sup> mice using alcian blue (cartilage) and alizarin red (bone) staining. Additional examples presented in support of results shown in Figure 5.**

**Figure S6.**



**Figure S6. Comparison of E18.5 hindlimb and pelvic bone morphology in wild type and PDE<sup>-/-</sup> mice. Additional examples presented in support of results shown in Figure 5.**